Available online at www.sciencedirect.com
ScienceDirect
Bioorganic & Medicinal Chemistry Letters
Bioorganic & Medicinal Chemistry Letters 17 (2007) 1793–1798

1,2,3-Thiadiazole substituted pyrazolones as potent KDR/VEGFR-2 kinase inhibitors

Rabindranath Tripathy,* Arup Ghose, Jasbir Singh, Edward R. Bacon, Thelma S. Angeles, Shi X. Yang, Mark S. Albom, Lisa D. Aimone, Joseph L. Herman and John P. Mallamo

Cephalon Inc., 145 Brandywine Parkway, West Chester, PA 19380, USA

Received 24 October 2006; revised 12 December 2006; accepted 13 December 2006
Available online 21 December 2006

Abstract—KDR kinase inhibition is considered to play an important role in regulating angiogenesis, which is vital for the survival and proliferation of tumor cells. Recently we disclosed a structure-based kinase inhibitor design strategy which led to the identification of a new class of VEGFR-2/KDR kinase inhibitors bearing heterocyclic substituted pyrazolones as the core template. Instability in a rat S9 preparation and poor iv PK profiles for most of these inhibitors necessitated exploration of new pyrazolones to identify new analogs with improved metabolic stability. Optimization of the heterocyclic moiety led to the identification of the thiadiazole series of pyrazolones (**D**) as potent VEGFR-2/KDR kinase inhibitors. SAR modifications, kinase selectivity profiling, and structural elements for improved PK properties were explored. Oral bioavailability up to 29% was achieved in the rat. Modeling results based on the Glide XP docking approach supported our postulation regarding the interaction of the lactam segment of the pyrazolones with the hinge region of the KDR kinase.

Identification of novel receptor tyrosine kinase (RTK) inhibitors continues to be an intense area of investigation in anti-tumor research,[1] due to the fact that overexpression of some of their corresponding receptor proteins contributes to constitutive RTK signaling, resulting in dysregulated cell growth and cancer.[2] Such uncontrolled RTK signaling leading to tumor growth has provided the impetus for the design of RTK inhibitors as potential anti-tumor agents. The approval of Sorafenib,[3a] Sunitinib,[3b] and Iressa[4] has validated such mechanistic approaches. One of the most extensively studied pathways in this area is vascular endothelial growth factor (VEGF)[5] and its cell surface receptor in human KDR (kinase domain containing receptor or VEGFR-2)[6] due to their important roles in angiogenesis[7] which is vital for survival and proliferation of tumor cells. KDR receptors, shown to be expressed primarily in endothelial cells,[8] upon binding to VEGF get activated and their intracellular kinase domains undergo autophosphorylation, which in turn triggers signaling pathways leading to sprouting of blood vessels toward the tumor cells. Therefore, inhibition of KDR kinase and subsequent blockage of angiogenesis could provide an alternate approach to cancer therapy.[9]

Recently, we disclosed the identification of a novel class of KDR kinase inhibitors (Fig. 1, **A** and **B**) comprising heterocyclic substituted pyrazolones as the core structure.[10] A structure-guided stepwise construction and exploitation of the Knoevenagel condensation[11] led us to the identification of this series of molecules. By appropriately modifying the heterocyclic moiety (with 1–2 heteroatoms) in **C**, coupled with versatility of the aldehydes, it was possible to generate an array of very potent and specific KDR kinase inhibitors. While the interaction of these inhibitors with the KDR protein at the molecular level is not fully understood, we proposed, on the basis of some structure–activity relationship (SAR) evidence, the structural elements essential for kinase binding, summarized in Figure 1 (**C**). A major liability of the pyrazolone series, however, was the metabolic instability of these compounds in rat liver S9 fraction in the presence of 2 mM NADPH.[12] Most of the compounds were not detected after 30 min of incubation. Pharmacokinetic (PK) profiles in the rat also showed similar trends and intravenous (iv) administra-

Keywords: KDR kinase; VEGFR-2 kinase; Kinase inhibitors; 1,2,3-Thiadiazole-pyrazolones.
* Corresponding author. Tel.: +1 610 738 6137; fax: +1 610 738 6558; e-mail: rtripath@cephalon.com

0960-894X/$ - see front matter © 2007 Elsevier Ltd. All rights reserved.
doi:10.1016/j.bmcl.2006.12.054

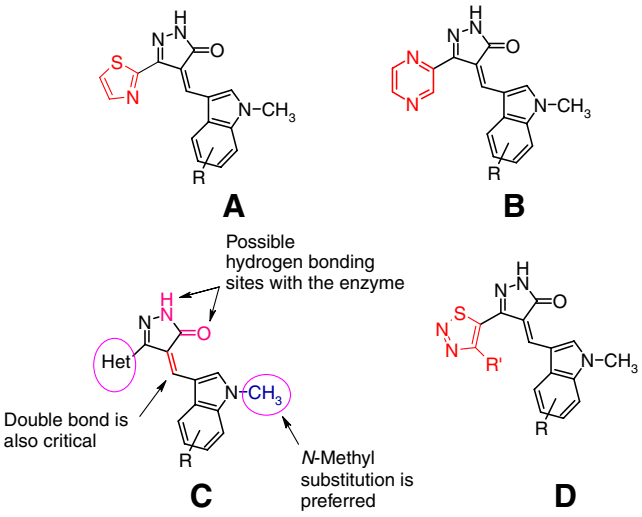

Figure 1. General structures of pyrazolone-based KDR kinase inhibitors (**A** and **B**); important structural features for activity (**C**) and general structure of the proposed pyrazolones bearing 1,2,3-thiadiazole (**D**).

tion of many of these compounds exhibited rapid clearance.[12] While the pyrazinyl derivatives (**B**, Fig. 1) were among the most potent KDR kinase inhibitors against the isolated enzyme and in cells,[10] members of this class were particularly vulnerable to metabolic instability in the S9 assay. However, one observation from the S9 incubation studies was that some of the indole derivatives which were inactive against KDR kinase were also resistant to in vitro metabolism. Encouraged by this observation, we further explored heterocyclic variations which ultimately led to the identification of 1,2,3-thiadiazole substituted class of pyrazolones (Fig. 1, **D**). Herein we disclose the synthesis, SAR, improved PK profile, and modeling results for this class of molecules.

Based on our earlier work,[10] different 1,2,3-thiadiazole-substituted pyrazolones and N-methyl-substituted indole 3-carboxaldehydes were easily synthesized as shown in Schemes 1–3. Methylthiadiazolepyrazolone (**3**) was synthesized in two steps starting from the commercially available 4-methyl[1,2,3]thiadiazole-5-carboxylic acid ethyl ester (**1**) in 50% overall yield via the β-ketoester intermediate **2** (Scheme 1).[13] Scheme 2 shows a representative example of the synthesis of *N*-methyl-indole-3-carboxaldehydes starting from 4-hydroxyindole (**4**). Selective ethyl protection of the hydroxyl group followed by Vilsmeier formylation at the 3-position of the indole gave compound **6** in 69% overall yield. Methylation of the indole nitrogen provided the N-methylated aldehyde **7** which was ready for Knoevenagel condensation. Other indole aldehydes were prepared in a similar fashion by using commercially available or literature-reported indoles. The condensation in each case was carried out by heating equimolar quantities of pyrazolone and aldehyde in ethanol in the presence of a catalytic amount of piperidine. Usually a precipitate is formed within a few minutes of heating, which upon filtration provides a single product[14] (**8k** is shown in Scheme 2) with high purity (>98%) in most of the cases. Such a facile work-up and simple purification technique allowed us to rapidly generate an array of compounds utilizing a variety of indole carboxaldehydes. On the other hand, Scheme 3 shows the synthesis of the unsubstituted pyrazolone **13**, for which the starting 1,2,3-thiadiazole 5-carboxylic acid ethyl ester (**12**) was prepared via semicarbazone **11**[15] followed by rearrangement to 1,2,3-thiadiazole in presence of thionyl chloride.[16] Subsequent β-ketoester formation followed by cyclization with hydrazine resulted in the pyrazolone **13**. Similar condensation with indole carboxaldehydes resulted in product **14** (**14l** is shown, Scheme 3).

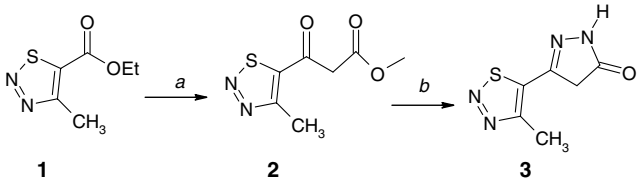

Scheme 1. Reagents and conditions: (a) NaH/methylacetate/reflux; (b) hydrazine hydrate/ EtOH/reflux, 50% in two steps.

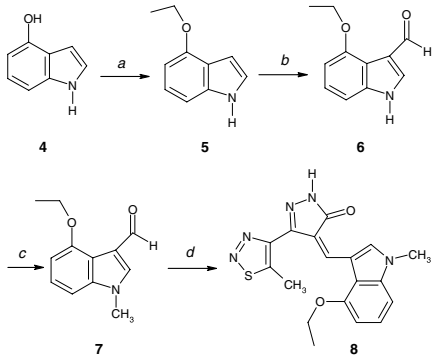

Scheme 2. Reagents and conditions: (a) Cs_2CO_3/EtI/acetone/reflux; (b) $POCl_3$/DMF, 0–60 °C, 69% in two steps; (c) NaH/MeI/DMF, 0 °C-rt, 75%; (d) **3**, EtOH/piperidine/heat, 82%.

Using our proposed mode of binding of pyrazolones (Fig. 1, **C**) with KDR kinase as a guide, we directed structural diversity in the thiadiazole series to various indole positions[17] and 4-substitution of the thiadiazole ring, respectively. The lactam unit, the exocyclic double bond remained intact. Similarly, the indole *N*-methyl group was thought to be optimal, and further variation of such group was not pursued.

Compounds generated were tested for their ability to inhibit the kinase activity of baculovirus-expressed human VEGFR-2 (KDR) cytoplasmic domain using time-resolved fluorescence (TRF) assay.[18] Table 1 highlights the SAR of methyl thiadiazoles **8** bearing 3-substituted indole moieties. These results corroborated our earlier observation that N-methylated indoles showed better activities than the corresponding N-unsubstituted indoles (Table 1, **8** and **8a**). While a variety of indole substituents at different positions were tolerated, most did not result in improved potency. The only exception was the indole-4 position, where substituents such as Cl,

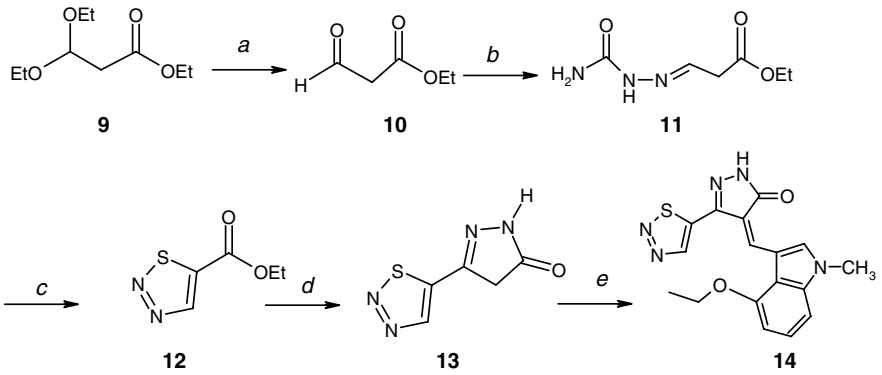

Scheme 3. Reagents and conditions: (a) dichloromethane: water/TFA; RT; (b) semicarbazide/NaOAc/water: EtOH, 58%; (c) $SOCl_2$, 0–60 °C, 67%; (d) i—NaH/Methylacetate/reflux, ii—Hydrazine hydrate/methanol/reflux, 22% in two steps; (e) **7**, EtOH/piperidine/heat, 48%.

Br, alkoxy, and methyl improved potency against KDR (Table 1, **8h**–**8l**). Inhibitors bearing *bis* substituents on the indole ring involving a 4-position also showed potency improvements (Table 1, **8m** and **8p**). Compounds showing <50 nM in vitro potency were tested in the human umbilical vein endothelial cell (HUVEC)-based phosphorylation assays and were found to be potent.

The KDR kinase inhibition results and HUVEC cell data for thiadiazoles lacking a 4-methyl group are listed in Table 2. These compounds were found to be generally more potent than the methylthiadiazoles. Substituents at

Table 1. Representative examples of KDR inhibitory activity of 4-methyl-1,2,3-thiadiazole-substituted pyrazolones (**8**–**8p**)

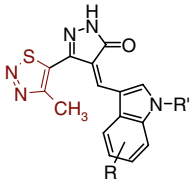

8

Compound[a]	R	R′	IC_{50}[b] (nM)	Cell score[c] (HUVEC)
8	H	H	>1000	—
8a	H	CH_3	95	0
8b	5-F	CH_3	99	—
8c	5-Cl	CH_3	152	—
8d	5-Cl	H	>300	—
8e	5-OCH3	CH_3	90	—
8f	5-CN	CH_3	>300	—
8g	4-F	CH_3	137	—
8h	4-Cl	CH_3	45	2
8i	4-Br	CH_3	34	3
8j	4-OCH_3	CH_3	19	4
8k	4-OCH_2H_5	CH_3	38	4
8l	4-CH3	CH_3	58	—
8m	4-Br,5-OCH_3	CH_3	23	4
8n	7-OCH_3	CH_3	109	—
8p	4,7-bis-OCH_3	CH_3	20	3

[a] A single geometrical isomer was isolated in each case. See Ref. 14.
[b] Ref. 18a.
[c] Ref. 18b.

Table 2. Representative SAR of 1,2,3-thiadiazole substituted pyrazolones-based KDR kinase Inhibitors (**14a-q**)

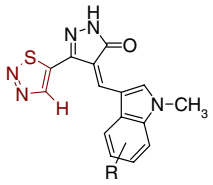

14

Compound[a]	R	IC_{50}[b] (nM)	Cell score[c] (HUVEC)
14a	5-F	48	1
14b	5-Cl	34	2
14c	5-CN	174	—
14d	5-$COOCH_3$	73	—
14e	5-OCH_3	28	3
14f	5-Br	110	—
14g	5-CH_3	35	4
14h	4-F	16	4
14i	4-Cl	16	2
14j	4-Br	8	1
14k	4-OCH_3	13	4
14l	4-OC_2H_5	25	4
14m	4-$COOCH_3$	22	3
14n	4-Br, 5-OCH_3	6	4
14o	6-Cl	73	—
14p	4-Br, 6-CH_3	12	0
14q	4,7-bis-OCH_3	10	4

[a] A single geometrical isomer was isolated in each case. See Ref. 14.
[b] Ref. 18a.
[c] Ref. 18b.

different positions on the indole-benzene ring were also tolerated. However, compounds bearing substituents such as 5-CN (**14c**), 5-$COOCH_3$ (**14d**), 5-Br (**14f**), and 6-Cl (**14o**) displayed IC_{50} values >50 nM. One interesting finding came from the 4-bromo-substituted pyrazolones (Table 2 **14j**, **14n**, **14p**). Although these compounds were potent against the isolated enzyme, this potency did not translate into cellular potency in at least two cases. In contrast, similar substitution translated to high potency in the pyrazine-pyrazolones (**B**), both in cells and against the isolated enzyme.[10] However, it was also found that irrespective of the nature of the heterocyclic group on the pyrazolones, 4-alkoxy substitution on the

indole segment (Table 1, **8J**, **8K**; Table 2, **14k**, **14l**; also Ref. 10) resulted in a good correlation between in vitro potency and cell permeability. Moreover, a promising PK profile also provided compelling reason to focus on 4-alkoxy indole substituted pyrazolones. Replacement of the 4-methyl group by phenyl[19a] in 1,2,3-thiadiazole resulted in approximately threefold loss in potency (Fig. 2, **15** and Table 1, **8i**). Similarly, switching to pyrroles (as in structure **16** and **17**, Fig. 2) in place of indoles, which are known and potent segments of pyrazolone-based kinase inhibitors,[10] also did not show dramatic improvement in potency against KDR kinase.[19b]

Selected compounds from both series (Tables 1 and 2) including compound **17** were tested for their intravenous (iv) PK profile in the rat. Unfortunately, like pyrazolones **A** and **B** (Fig. 1) most of the compounds demonstrated very low plasma levels, high clearance rates (CL), and resulting short half-lives ($t_{1/2}$). Some of the methylthiadiazoles showed improved PK profiles compared to their unsubstituted counterparts. More importantly, structural changes within the methylthiadiazole series played an important role in improving the PK profile. For example, simple exchange of the 4-methoxy (**8j**) to 4-ethoxy on the indole ring (**8k**) significantly improved the iv PK profile in the rat (Table 3, Fig. 4). Another encouraging example was methylthiadiazole compound **8b** (Figs. 3, 4). By blocking a possible metabolic site on the indole 5-position (5-H replaced with 5-F), the iv PK profile was improved significantly. More strikingly, this compound also demonstrated 29% oral bioavailability (BA) after a 5 mg/kg po dose in the rat (Figs. 3, 4). Despite modest potency for **8b** and poor cell permeability, we selected this compound for PK profiling as a proof-of-concept molecule based on favorable iv PK data previously obtained with an analogous compound (**A-1**, R = F, Figs. 3 and 4) in the thiazole series, bearing a 5-fluoroindole group (Table 3). However, **A-1** showed low oral bioavailability (~3%). Therefore, a methylthiadiazole substituent on the pyrazolone ring showed better bioavailability than the corresponding thiazole-based pyrazolone, at least in a comparable system. Figure 4 summarizes the PK results.

Table 4 shows the selectivity profile of a representative inhibitor, **8k**, against a panel of tyrosine kinases. **8k** demonstrates potent, low-nanomolar inhibition of KDR, VEGFR3, TRK A, and FLT3. Other kinases such as SRC, VEGFR1, c-Met, and Tie-2 are only weakly inhibited.

Table 3. IV and oral PK profile of selected pyrazolones in the rat

Compound	Intrinsic (iv) Pharmacokinetics in rat[a]			
	AUC (ng*h/mL)	T1/2 (h)	Vd (L/kg)	CL (mL/min/kg)
8j	192	0.3	2.2	87
8k	1141	0.9	1.1	15
8b	727	0.5	1.1	25
8b (Oral)[b]	1042	1.2	—	—
A-1 (R = F)	3599	0.6	0.23	4.6
A-1 (Oral)[c]	507	1.4	—	—

[a] iv dosing was at 1 mg/kg (using 3% DMSO, 30% Solutol, and 67% phosphate-buffered saline (PBS) as the vehicle, Pharmacokinetic parameters were estimated for each rat by non-compartmental analysis of the plasma concentration versus time data using WinNonlin software (Professional Version 2.1, Pharsight Corporation, Palo Alto, CA, 1997).

[b] Oral dosing was at 5 mg/kg, C_{max} = 356 ng/mL (using 50% Tween 80, 40% propylene carbonate, and 10% propylene glycol).

[c] Oral dosing was at 5 mg/kg, C_{max} = 139 ng/mL (using 50% Tween 80, 40% propylene carbonate, and 10% propylene glycol).

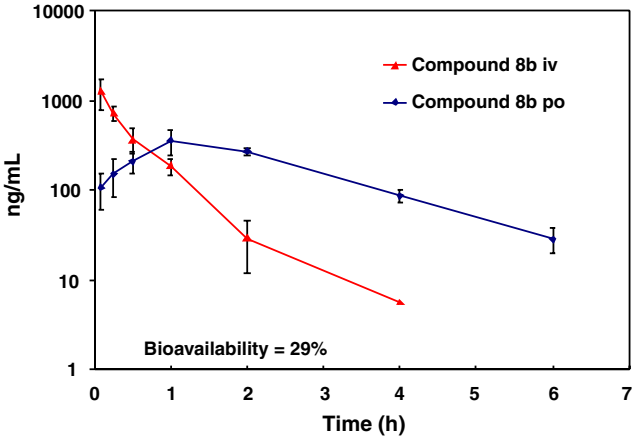

Figure 3. Plasma levels of compound **8b** in the rat (1 mg/kg iv, 5 mg/kg po).

Modeling results based on the Glide XP docking approach[20] supported our postulation regarding interaction of the lactam segment of the pyrazolones with the hinge region of the KDR kinase. The lactam ring of the pyrazolone has one hydrogen donor NH flanked by two hydrogen acceptors, that is, the carbonyl O and N. This may lead to two possible binding modes of the pyrazolone ring in the hinge region: either the hydrogen acceptor O or the N may bind with the

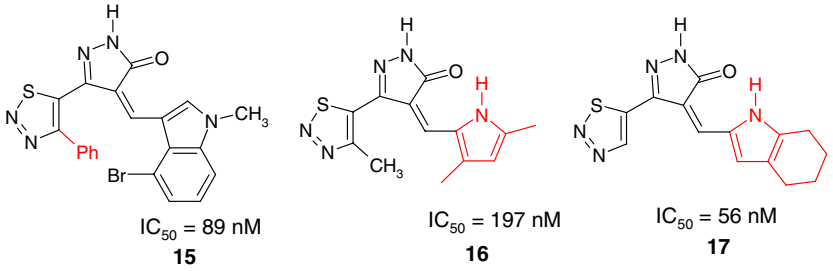

Figure 2. KDR kinase binding results of pyrazolones: (a) 4-phenyl thiadiazole (**15**); (b) thiadiazoles bearing pyrrole segments (**16**, **17**).

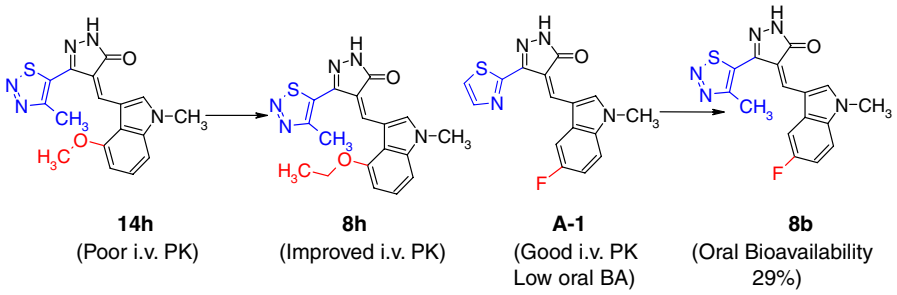

Figure 4. Summary of structural modifications to improve PK.

Table 4. Kinase inhibition profiles of the pyrazolone **8k**

Kinase	IC_{50}(nM)	Kinase	IC_{50}(nM)
KDR	38	Tie-2	>10000
VEGFR1	>3000	c-Met	3700
VEGFR3	16	TRK A	36
SRC	463	FLT3	19

Cys-917 backbone NH. There are four VEGFR-2 structures in the protein databank (1VR2, 1Y6A, 1Y6B, and 1YWN). 1VR2 is the apo-protein structure; 1YWN has a ligand bound DFG-out structure. The other two were intermediate structures where the Phe of DFG was neither 'in' nor 'out'. To understand the binding modes of these pyrazolones, we used Glide XP docking approach and the 1Y6B structure.

During the 'protein preparation' however, the missing part of the P-loop (Ala-842 and Phe-843) was built, following the conformation of 1YWN, followed by a constrained minimization. The Glide docking study also showed two major binding modes as discussed above. The most frequently occurring binding mode had the pyrazolone O bound to the Cys-917 NH and the thiadiazole ring near the salt bridge Lys-866 (Fig. 5). These studies revealed no clear SAR to differentiate between the two binding modes. It is also possible that the nature of substitution may dictate one over the other.

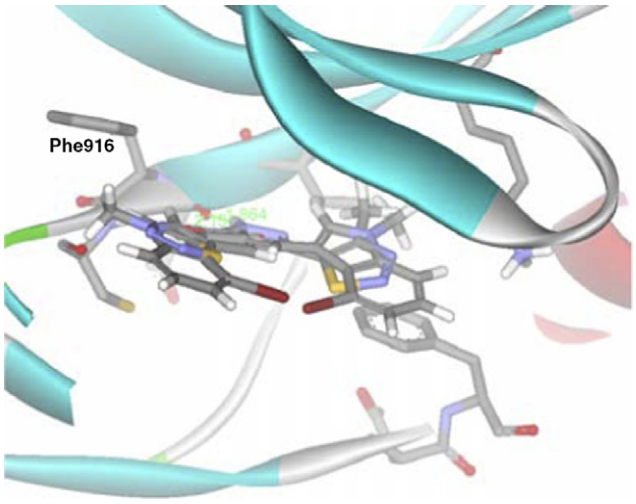

Figure 5. The two possible binding modes often found by Glide for the various pyrazolones. The distance of the pyrazolone NH from the Glu-915 (CO) was 1.86A in the more frequent binding mode.

In conclusion, we have identified two series of 1,2,3-thiadiazole substituted pyrazolones as potent and cell-permeable KDR kinase inhibitors. Although 4-methyl substituted thiadiazolepyrazolones were less robust in potency than their unsubstituted counterpart, they showed an improved PK profile. We have identified structural moieties (4-ethoxy, 5-fluoro on the indole ring) responsible for improved iv PK profile in the rat. Compound **8b** showed 29% oral bioavailability in rats. Modeling results supported the hypothesis regarding the mode of interaction of pyrazolone-based inhibitors with KDR kinase. Anti-tumor properties from this class of molecules will be reported in due course.

Acknowledgments

We thank Kurt A. Josef for his help in NMR experiments, Sheryl L. Meyer, and Chrysanthe M. Spais for providing purified recombinant proteins.

References and notes

1. For reviews, see (a) Bouïs, D.; Kusumanto, Y.; Meijer, C.; Mulder, N. H.; Hosper, G. A. P. *Pharmacol. Res.* **2006**, *53*, 89; (b) Kim, D. N.; Lu, B.; Hallahan, D. E. *Curr. Opin. Investig. Drugs* **2004**, *5*, 597; (c) Cohen, P. *Curr. Opin. Chem. Biol.* **1999**, *3*, 459.
2. (a) Bennasroune, A.; Gardin, A.; Aunis, D.; Crémel, G.; Hubert, P. *Critical Rev. Oncol./Hematol.* **2004**, *50*, 23; (b) Christensen, J. G.; Schreck, R.; Burrows, J.; Kuruganti, P.; Chan, E.; Le, P.; Chen, J.; Wang, X.; Ruslim, L.; Blake, R.; Lipson, K. E.; Ramphal, J.; Do, S.; Cui, J. J.; Cherrington, J. M.; Mendel, D. B. *Cancer Res.* **2003**, *63*, 7345.
3. (a) Wilhelm, S.; Carter, C.; Lynch, M.; Lowinger, T.; Dumas, J.; Smith, R. A.; Schwartz, B.; Simantov, R.; Kelley, S. *Nat. Rev. Drug Discov.* **2006**, *5*, 835; (b) Cabebe, E.; Wakelee, H. *Drugs Today (Barc)* **2006**, *42*, 387.
4. McKillop, D.; Partridge, E. A.; Kemp, J. V.; Spence, M. P.; Kendrew, J.; Barnett, S.; Wood, P. G.; Giles, P. B.; Patterson, A. B.; Bichat, F.; Guilbaud, N.; Stephens, T. C. *Mol. Cancer Ther.* **2005**, *4*, 641.
5. Jakeman, L. B.; Armanini, M.; Phillips, H. S.; Ferrara, N. *Endocrinology* **1993**, *133*, 848.
6. (a) De Vries, C.; Escobedo, J. A.; Ueno, H.; Houck, K.; Ferrara, N.; Williams, L. T. *Science* **1992**, *255*, 989; (b) Terman, B. I.; Dougher-Vermazen, M.; Carrion, M. E.; Dimitrov, D.; Armellino, D. C.; Gospodarowicz, D.; Bohlen, P. *Biochem. Biophys. Res. Commun.* **1992**, *187*, 1579.

7. Klagsbrun, M.; Moses, M. A. *Chem. Biol.* **1999**, *6*, R217.
8. Strawn, L. M.; McMahon, G.; App, H.; Schreck, R.; Kuchler, W. R.; Longhi, M. P.; Hui, T. H.; Tang, C.; Levitzki, A.; Gazit, A.; Chen, I.; Keri, G.; Orfi, L.; Risau, W.; Flamme, I.; Ullrich, A.; Hirth, K. P.; Shawver, L. K. *Cancer Res.* **1996**, *56*, 3540.
9. Paz, K.; Zhu, Z. *Front. Biosci.* **2005**, *10*, 1415.
10. Tripathy, R.; Reiboldt, A.; Messina, P. A.; Iqbal, M.; Singh, J.; Bacon, E. R.; Angeles, T. S.; Yang, S. X.; Albom, M. S.; Robinson, C.; Chang, H.; Ruggeri, B. A.; Mallamo, J. P. *Bioorgan. Med. Chem. Lett.* **2006**, *16*, 2158.
11. March, J. In *Advance Organic Chemistry*, 3rd ed.; John Wiley & Sons, Inc.: New York, 1985; p 835.
12. Unpublished results.
13. Battegay, M.; Wolff, A. *Bull. Soc. Chim.* **1923**, *33*, 1481.
14. The configuration of the double bond is assumed to be *Z* in all cases based on ^{1}H-NMR chemical shift correlations and x-structure of a related pyrazolone (see Ref. 10).
15. Wisliconus, W. *Justus Liebigs Ann. Chem.* **1907**, *356*, 46.
16. Shafiee, A.; Lalezari, I.; Mirrashed, M.; Nercesian, D. *J. Heterocyclic Chem.* **1977**, *14*, 567, and references there in.
17. Indole-2- position was not explored, as a methyl substituent in the pyrazine series (**B-1**, R = 2-methyl) was not tolerated (only 7% inh. at 300 nM), whereas the desmethyl compound, **B-2**, R = H, had an IC_{50} value of 37 nM against KDR[10].
18. (a) The VEGFR-2/KDR assay was performed in a microtiter plate format using time-resolved fluorescence (TRF). Briefly, each 96-well plate (Costar # 3922; Corning, NY) was coated with 20 μg/mL of substrate solution (recombinant human GST-PLC-γ/GST) in Tris-buffered saline (TBS). The KDR assay mixture (total volume = 100 μL/well) containing 20 mM Hepes, pH 7.2, 40 μM ATP, 10 mM $MnCl_2$, 0.1% BSA, and variable concentrations of test compound (diluted in DMSO; 2.5% DMSO final in assay) was then added to the assay plate. Enzyme (30 ng/mL KDR) was added and the reaction was allowed to proceed at 37 °C for 15 min. The phosphorylated product was detected by incubating with Eu-N1-labeled PY100 antibody (Perkin–Elmer Life Sciences #AD0160, Boston, MA) at 37 °C for 1 h, followed by addition of enhancement solution (Perkin–Elmer Life Sciences #1244-105, Boston, MA). After a few minutes, the fluorescence of the resulting solution was measured using the Perkin–Elmer EnVision 2100 (or 2102) multilabel plate reader. Inhibition data were analyzed using IDBS ActivityBase and IC_{50} curves were generated using XLFit 3. IC_{50} values were reported as the average of at least two independent determinations.; (b) Subconfluent HUVECs were serum-starved by replacing media with EBM-2 (endothelial cell basal medium, serum-free; Clonetics #CC-3156; BioWhittaker, Walkersville, MD) containing 0.05% BSA for 1 h at 37 °C, during which time the test compound (50 nM) or DMSO (control) was added to the cells. Human VEGF (Clonetics #CC-4114) was then added to the cells at a concentration of 10 ng/mL for 5 min. Cells were lysed in radioimmunoprecipitation assay (RIPA) buffer containing 1 mM activated sodium vanadate and protease inhibitors (Protease Inhibitor Cocktail Set III; Calbiochem, San Diego, CA), sheared with a 27 gauge syringe, and then centrifuged at 12,000*g* for 15 min. Clarified cell lysates were immunoprecipitated with anti-VEGFR-2 antibody for 1 h, followed by incubation with Protein A Sepharose for another hour at 4 °C and analysis by SDS–PAGE. Western blotting was performed using 4G10 anti-phosphotyrosine antibody (Upstate #05-321; Lake Placid, NY) and phosphorylated proteins were visualized using enhanced chemiluminescence (ECL) (Amersham #RPN2106, Piscataway, NJ). The percentage inhibition was calculated by analyzing scanned autoradiographs on a densitometer. Scores were based on decrease in protein band density compared with VEGF-stimulated control (no inhibitor) as follows: 0 = no decrease; 1 = 1–25%; 2 = 26–50%; 3 = 51–75%; 4 = 76–100%.
19. (a) The pyrazolone precursor for **15**[16] was prepared in a similar method as outlined in Scheme 3.; (b) The inhibitors **16** and **17** were prepared by the condensation of 3,5-dimethyl-1*H*-pyrrole-2-carboxaldehydealdehyde and 4,5,6,7-tetrahydroindole-2-carboxaldehyde with the pyrazolones **3** and **13**, respectively.
20. Friesner, R. A.; Banks, J. L.; Murphy, R. B.; Halgren, T. A.; Klicic, J. J.; Mainz, D. T.; Repasky, M. P.; Knoll, E. H.; Shelley, M.; Perry, J. K.; Shaw, D. E.; Francis, P.; Shenkin, P. S. *J. Med. Chem.* **2004**, *47*, 1739.